Photoassisted Decomposition of Malonic Acid on TiO_2 Studied by in Situ Attenuated Total Reflection Infrared Spectroscopy

Igor Dolamic and Thomas Bürgi*

Université de Neuchâtel, Institut de Microtechnique, Rue Emile-Argand 11, 2009 Neuchâtel, Switzerland

Received: March 18, 2006; In Final Form: May 24, 2006

The photoassisted mineralization, i.e., conversion to CO_2 and water, of malonic acid over P25 TiO_2 was investigated by in situ attenuated total reflection infrared (ATR-IR) spectroscopy in a small volume flow-through cell. Reassignment of the vibrational bands of adsorbed malonic acid, assisted by deuterium labeling, reveals two dissimilar carboxylate groups within the molecule. This indicates adsorption via both carboxylate groups, one in a bridging or bidentate and the other in monodentate coordination. During irradiation the coverage of malonic acid strongly decreases, and oxalate is observed on the surface in at least two different adsorption modes. The major oxalate species observed during irradiation is characterized by monodentate coordination of both carboxylate groups. In the dark, however, part of these species adopts another adsorption mode, possibly interacting only with one carboxylate group. During band gap illumination a large fraction of the surface is not covered by acid. Oxalate is a major intermediate in the mineralization of malonic acid. However, the observed transient kinetics of adsorbed malonic and oxalic acid indicates additional pathways not involving oxalate. The rate constant for oxalate decomposition is slightly larger than the one for oxalate formation from malonic acid. As the oxalate is desorbing slowly from the surface its concentration in the liquid phase is small, despite the fact that it is a major intermediate in the mineralization of malonic acid.

Introduction

Photoassisted reactions on TiO_2 particles have attracted much interest due to promising applications in solar energy conversion (water splitting)[1,2] and environmental cleaning, i.e., decomposition of organic pollutants in gaseous effluents and wastewater.[3−5] The latter two processes may largely contribute to future sustainable technologies. Upon excitation of TiO_2 across the band gap an electron−hole pair is generated.[6] It is believed that these electrons and holes can be trapped at Ti(IV)O−H surface sites, leading to $Ti(III)O-H^-$ and $Ti(IV)O^{\bullet}-H^+$, respectively.[7] The photoassisted degradation of organic molecules adsorbed on Ti sites can be initiated by their direct reaction with photogenerated holes, i.e., electron vacancies in the valence band of the semiconductor,[8] which leads to highly reactive species. This is likely the predominant mechanism for organic anions that strongly adsorb on the TiO_2 surface.[9] Alternatively, O−H radicals generated by the trapped holes may initiate reaction. The trapped electrons are believed to react with adsorbed oxygen, leading to O_2^- and O_2^{2-} species that may also contribute to the oxidation of organic compounds.

As most studies have focused on the analysis of stable reaction intermediates (in the gas or liquid phase) the fate of the organic reactants on the TiO_2 surface remains unclear. In fact, only a few studies were reported that give direct spectroscopic information on the composition of the adsorbate layer during or after photoreaction. Attenuated total reflection infrared (ATR-IR) spectroscopy[10] is a powerful tool to study the solid−liquid interface of powders,[11−13] and it has also been applied to study catalytic reactions.[14−24] ATR-IR spectroscopy has recently also been used to study band gap irradiation of TiO_2 particle films in contact with water. Vibrational bands below 1000 cm^{-1} that appeared upon irradiation were assigned to surface peroxo and hydroperoxo species.[25,26] In another ATR-IR study the influence of adsorbed water on TiO_2 was investigated.[27] When removing water several bands below 1000 cm^{-1} appeared under near-UV irradiation.

Studies that directly address the fate of molecules adsorbed on the TiO_2 surface upon UV exposure are rare. The photodegradation of 4,4′-bis(2-sulfostyryl)biphenyl was followed by ATR-IR.[28] The adsorption and photoassisted reaction of glyoxylic acid on TiO_2 was studied.[29] Glyoxylic acid (HCO−COOH) exists in aqueous solutions as the hydrated *gem*-diol and most likely adsorbs on TiO_2 through bidentate chelation to Ti via carboxylate and hydroxylate.[29] Upon band gap irradiation this species is transformed to oxalate. The photoassisted reaction of oxalic acid[30,31] and catechol[30] on TiO_2 was also probed by ATR-IR spectroscopy. Upon irradiation the adsorbed catechol is depleted, and evidence was given for carbonate formation. Oxalic acid adsorbs in three different modes on TiO_2 surfaces.[11] On the basis of kinetic analysis it was concluded that upon irradiation the two less stable adsorption modes transform into the most stable adsorbed species, which is the most photolabile and reacts to CO_2.[31]

Here we report the photoassisted degradation of malonic acid on TiO_2 as studied by in situ ATR-IR spectroscopy. In contrast to oxalic acid (HOOC−COOH), which is easily oxidized to two CO_2 molecules, the photoreaction of malonic acid is expected to proceed in several consecutive steps. This opens up the possibility to detect intermediate adsorbed species and therefore to shed light on the reaction pathway.

Experimental Section

Catalyst and Chemicals. Degussa P25 TiO_2, containing 80% anatase and 20% rutile with a surface area of 51 $m^2\ g^{-1}$ and average primary particle size of 21 nm, was used in the

* Corresponding author. Phone: ++41 32 718 24 12. Fax: ++41 32 718 25 11. E-mail: thomas.burgi@unine.ch.

10.1021/jp0616967 CCC: $33.50
Published on Web 07/07/2006

photoassisted reactions. Malonic acid (Sigma-Aldrich, 99%), d_4-malonic acid (Aldrich, 99+ atom % D), sodium hydroxide (Sigma-Aldrich, 97%), and deuterium oxide (Aldrich, D-99.9%) were used as received.

Thin Film Preparation. A slurry of the catalysts powder was prepared from about 20 mg of catalyst and 25 mL of water (Milli-Q, 18 MΩ·cm). After sonication (ultrasonic cleaner, Branson 200) for 30 min TiO_2 thin films were formed by dropping the slurry onto a Ge internal reflection element (IRE) (52 mm × 20 mm × 1 mm; KOMPLAS). The amount of slurry for one coating was 0.5 mL. The solvent was allowed to evaporate, and the procedure was repeated two times. After drying for several minutes at 40 °C in air, loose catalyst particles were removed by flowing water over the IRE. After drying in air the film was ready for use. From the amount of deposited TiO_2 and its density an average film thickness of 4 μm was estimated. ZnSe IREs were also used for these types of experiments. However, upon irradiation some degradation of the ZnSe crystal was observed, resulting in a precipitate, likely Se^0, on the ZnSe crystal and a pH increase in reactant solution.[31]

ATR-IR Spectroscopy. ATR spectra were recorded with a dedicated flow-through cell, made from a Teflon piece, a fused silica plate (45 mm × 35 mm × 3 mm) with holes for the inlet and outlet (36 mm apart), and a flat (1 mm) viton seal. The cell was mounted on an attachment for ATR measurements within the sample compartment of a Bruker Equinox-55 FTIR spectrometer equipped with a narrow-band MCT detector. Spectra were recorded at 4 cm^{-1}. The reactant was passed through the cell and over the catalyst at a flow rate of 0.2 mL/min by means of a peristaltic pump (Ismatec, Reglo 100) located in front of the cell. Solutions of malonic acid (10^{-4} mol/L, pH about 3.5) were flowed over the TiO_2 film in the dark for 30 min in order to reach equilibrium. The pK_a values of malonic acid are 2.84 and 5.79.[32] Irradiation of the sample with UV light was carried out using a 75 W Xe arc lamp. The UV light from the source is guided to the cell via two fiber bundles. The light was passed through a 5 cm water filter to remove any infrared radiation. A Schott UG 11 (50 mm × 50 mm × 1 mm) broadband filter from ITOS was used to remove visible light (transmission between 270 and 380 nm). An estimate based on the supplier specifications gave a power at the sample of slightly less than 10 mW/cm^2. All experiments were performed at room temperature. A schematic of the experimental setup is given in Figure 1.

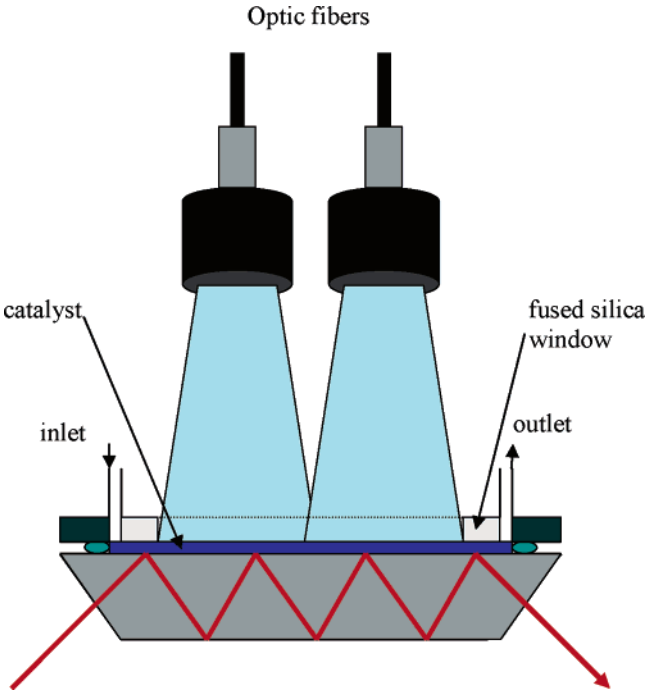

Figure 1. Schematic setup for in situ ATR-IR spectroscopy of photoassisted reactions in a small volume flow-through cell.

Results

ATR-IR Spectra of Dissolved and Adsorbed Malonic Acid on TiO_2. Figure 2 shows ATR-IR spectra of dissolved malonic acid, both in its protonated (b) and deprotonated state (a), and of malonic acid adsorbed from a diluted solution on a TiO_2 film (c). The spectra are in good agreement with previous reports.[33] The most prominent band of protonated malonic acid is associated with the ν(C═O) vibration at 1718 cm^{-1}. In the spectrum of the dissolved deprotonated acid the $\nu_{as}(COO^-)$ and $\nu_s(COO^-)$ modes at 1564 and 1355 cm^{-1} are the most intense. Weaker modes at 1437 and 1258 cm^{-1} were previously assigned to $\delta(CH_2)$ vibrations.[33] Upon adsorption from solution (Figure 2c) the molecule is deprotonated as evidenced by the broad $\nu_{as}(COO^-)$ band at 1600 cm^{-1}.

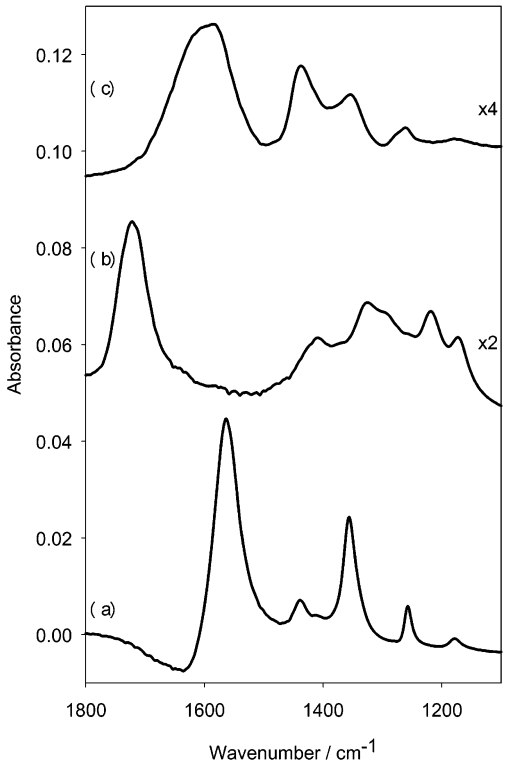

Figure 2. ATR-IR spectra of dissolved malonic acid and malonic acid adsorbed on TiO_2. (a) Malonic acid, 0.1 mol/L, in water at pH 8.6. The pH was adjusted with NaOH. Water served as the reference at the same pH. (b) Malonic acid, 0.1 mol/L, in water (pH = 1.5, no addition of NaOH). Pure water served as the reference. (c) Malonic acid adsorbed on a TiO_2 film. The spectrum was recorded while flowing a solution of 10^{-4} mol/L malonic acid over the film and represents the equilibrium state reached after about 30 min of contact. The TiO_2 film in contact with pure water served as the reference. The spectra are shifted for clarity. The negative band in spectrum (a) slightly above 1600 cm^{-1} is due to an incompensation of bulk water.

Figure 3 shows infrared spectra of malonic acid adsorbed on the TiO_2 film measured under different conditions. Spectrum (a) refers to adsorbed malonic acid in the dark. Spectra (b) and (c) were recorded under UV irradiation and while flowing a solution of malonic acid (10^{-4} mol/L) over the TiO_2 film. Under irradiation the bands of adsorbed malonic acid decrease. Concomitantly other bands increase, notably at 1708, 1690,

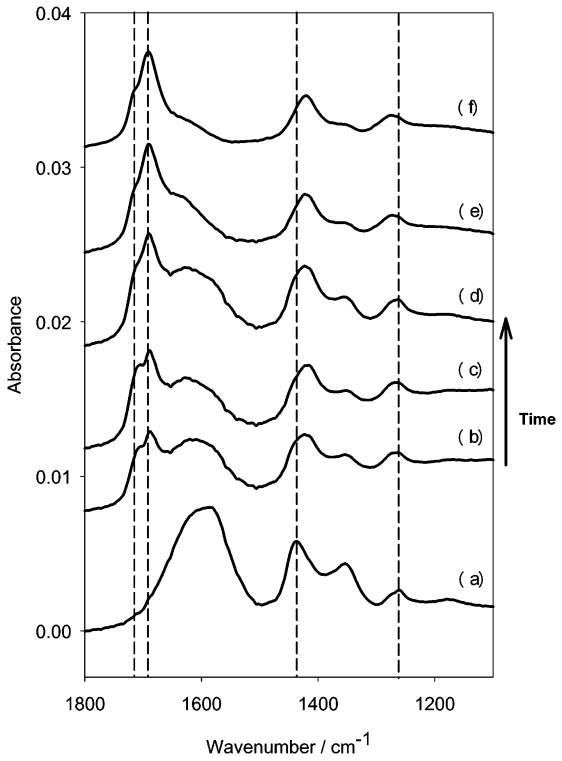

Figure 3. Series of ATR-IR spectra of malonic acid on TiO_2. The reference spectrum was recorded while flowing pure water over the TiO_2 film. Spectrum (a) was recorded in the dark while a solution of malonic acid (10^{-4} mol/L) was flowing over the TiO_2 film. Spectra (b) and (c) were recorded while illuminating the TiO_2 film and simultaneously flowing malonic acid solution (10^{-4} mol/L). Spectra (b) and (c) were recorded 7 and 20 min, respectively, after switching on the UV light. Spectra (d)−(f) were subsequently recorded in the dark while flowing pure water over the TiO_2 film. Spectra are offset for clarity. The vertical lines are just to guide the eye.

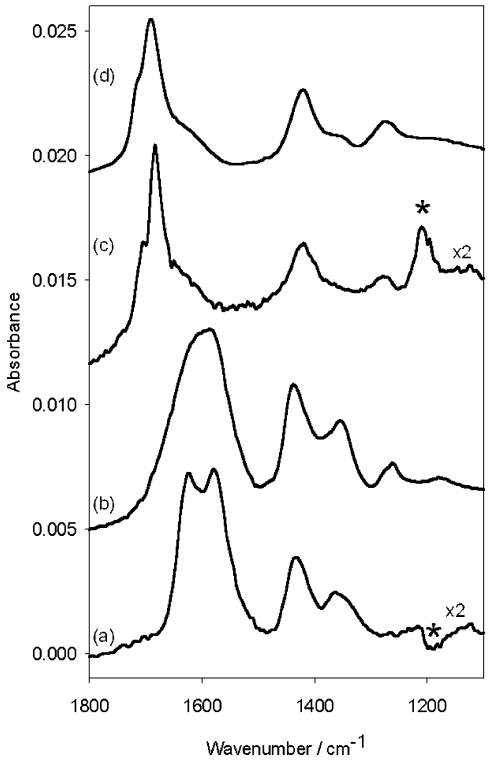

Figure 4. ATR-IR spectra of (a) d_4-malonic acid on TiO_2 adsorbed from D_2O, (b) malonic acid on TiO_2 adsorbed from H_2O, (c) d_4-malonic acid on TiO_2 after illumination and washing with D_2O, and (d) malonic acid on TiO_2 after illumination and washing with H_2O. Asterisks (∗) mark signals from uncompensated D_2O solvent.

1421, and 1275 cm^{-1}. After about 20 min the spectrum hardly changes anymore. It should be noted that under illumination a broad absorption was observed, extending from above 2000 to below 900 cm^{-1} and exponentially increasing at lower wavenumbers. Part of the intensity of this absorption increased/decreased abruptly upon turning the light on/off. Part of the absorbance showed slower response. A similar broad absorption was reported when irradiating dry TiO_2 films and was ascribed to an excitation of electrons from shallow traps to the conduction band of the TiO_2 semiconductor.[27] Alternatively, the broad band could be due to a scattering effect. Spectra (d)−(f) were recorded in the dark and while flowing neat water over the TiO_2 film. This leads to a desorption of the adsorbed malonic acid, leaving behind on the TiO_2 surface the species that were formed during illumination.

Figure 4 shows spectra for an analogous experiment as the one in Figure 3 but with deuterated malonic acid (d_4-malonic acid) in D_2O. The CH_2 vibrations in malonic acid strongly shift to lower wavenumbers in d_4-malonic acid. This is evident for the vibration at 1260 cm^{-1}, for the normal malonic acid (spectrum (b) in Figure 4), which was assigned to a CH_2 wagging mode.[33,34] In the corresponding spectrum of deuterated malonic acid (spectrum (a) in Figure 4) no band is observed at 1260 cm^{-1}. However, the species that is formed during illumination is not affected by deuteration (compare spectra (c) and (d) in Figure 4).

Figure 5 shows the time dependence of two signals at 1350 and 1708 cm^{-1} in the ATR-IR spectra. The former signal is associated with the $\nu_s(COO^-)$ mode of malonic acid adsorbed on TiO_2, whereas the latter can be assigned to $\nu(C{=}O)$ vibrations of the species that are formed under irradiation. The lines at the top of the figure indicate the state of the two parameters that were changed during the course of the experiment, namely, the UV light (on or off) and the concentration of malonic acid in solution (0 or 1.5×10^{-4} mol/L). First malonic acid is adsorbed in the dark (regime 1 in Figure 5). After reaching equilibrium the light is switched on (regime 2), which leads to a fast decrease of the amount of adsorbed malonic acid (signal at 1350 cm^{-1}). The latter reached a new stable level after about 5 min. Upon illumination the species associated with the 1708 cm^{-1} band appears. Figure 5 reveals that the disappearance of the 1350 cm^{-1} band is faster than the appearance of the 1708 cm^{-1} signal. Upon switching off the light again (regime 3 in Figure 5) malonic acid readsorbs fast. At the same time a slight increase of the absorbance at 1708 cm^{-1} is also observed. The subsequent flow of neat water in the dark (regime 4 in Figure 5) removes almost all malonic acid within about 15 min. The absorbance at 1708 cm^{-1} initially decreases fast and keeps decreasing further but at a much slower rate after about 5 min. When switching on the light again (regime 5 in Figure 5) the species associated with the 1708 cm^{-1} band vanishes initially very fast and later disappears completely, however, at a considerably slower rate. Illumination after readsorption (regime 7 in Figure 5) again leads to depletion of malonic acid on the surface and formation of the 1708 cm^{-1} signal (analogous as observed for treatment 2 in Figure 5). The small increase of the absorbance at 1708 cm^{-1} observed upon readsorption of malonic acid in the dark (regime 6 in Figure 5) can be attributed to the broad band of malonic acid centered around 1600 cm^{-1}, which has a tail above 1700 cm^{-1} (see also the difference spectra in Figure 6).

Figure 6 shows difference spectra for the same experiment as shown in Figure 5. The difference spectra reveal the spectral

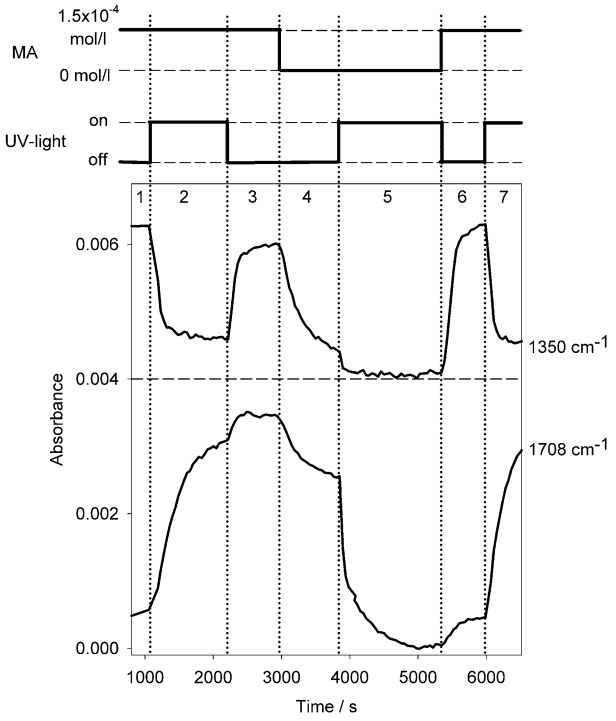

Figure 5. Absorbance at 1350 and 1708 cm^{-1} as a function of time as followed by ATR-IR spectroscopy during different treatments of a TiO_2 film with UV light and malonic acid solution. The state of the two parameters that were changed during the experiment, the UV light and the concentration of the malonic acid in solution, are given in the upper part of the figure. Regimes that correspond to a certain state of the two parameters are numbered consecutively. To get rid of drifts during the long experiment the two absorption signals were baseline corrected by subtracting the signal from a nearby spectral region with no absorption bands (1742 and 1315 cm^{-1}). The 1350 cm^{-1} signal was shifted by 0.004 for clarity.

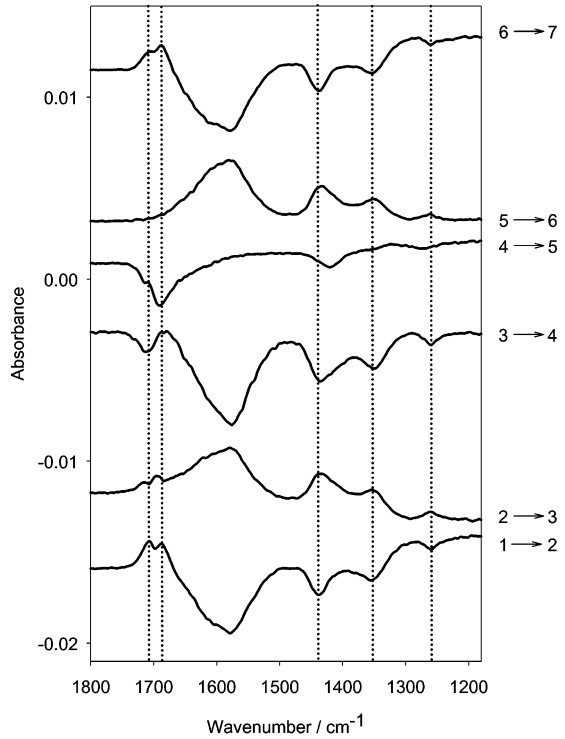

Figure 6. ATR-IR difference spectra for the same experiment as described in Figure 5. The numbers and arrows on the right side of the figure denote the two regimes, as described in Figure 5, that were used to calculate the difference spectrum. For example, 1 → 2 refers to a difference spectrum between the last spectrum recorded in regime 1 (flowing malonic acid over the surface in the dark) and one of the first spectra recorded in regime 2 (flowing malonic acid and turning on the UV light). Vertical lines are just to guide the eye.

changes observed upon changing conditions. For example, upon illumination (difference spectrum 1 → 2) the bands of adsorbed malonic acid appear negative, because the malonic acid coverage is decreasing. At the same time two positive bands at 1708 and 1690 cm^{-1} indicate the appearance of a new species containing C═O groups.

Figure 7 shows difference spectra recorded during illumination of the adsorbed species that is formed upon illumination of malonic acid, i.e., after illumination and desorption of unreacted malonic acid. (corresponding to regime 5 in Figure 5). Spectrum (a) refers to the spectral changes during the first 2 min (steep initial decrease in Figure 5, regime 5), spectrum (b) corresponds to the spectral changes of the subsequent 5 min, and spectrum (c) shows the changes during the subsequent 20 min. The spectra change qualitatively with time, which reveals that more than one species are involved in the process.

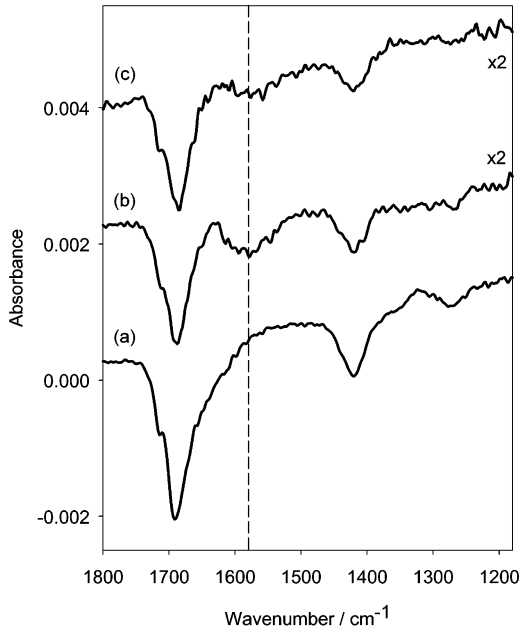

Figure 7. ATR-IR difference spectra for the same experiment as described in Figures 5 and 6. The spectra were recorded during illumination in water of a TiO_2 film that contained mainly adsorbed oxalic acid (regime 5 in Figure 5). Difference spectrum (a) reveals the changes during the first 2 min of illumination; difference spectrum (b) reveals the changes during the subsequent 5 min of illumination; difference spectrum (c) reveals the changes during the subsequent 20 min of illumination.

Discussion

Identification of the Species Absorbing at 1708 cm^{-1}. Figure 4 clearly shows that the spectrum of the species formed during irradiation does not change upon deuteration. It is therefore concluded that the new species does not contain hydrogen (deuterium) and consequently is composed of oxygen and carbon atoms only. Adsorbed oxalic acid, more precisely oxalate $^{-}OOC-COO^{-}$ is a feasible possibility.

Adsorption of oxalic acid from aqueous solutions on TiO_2 surfaces was investigated before by ATR-IR spectroscopy.[11,31] From the coverage-dependent spectral changes it was shown that several surface oxalate complexes coexist. With the use of singular value decomposition the spectra of three different components could be determined. The spectrum of the most

CHART 1: Different Adsorption Modes of Oxalate on TiO_2 and Proposed Adsorption Mode of Malonate on TiO_2

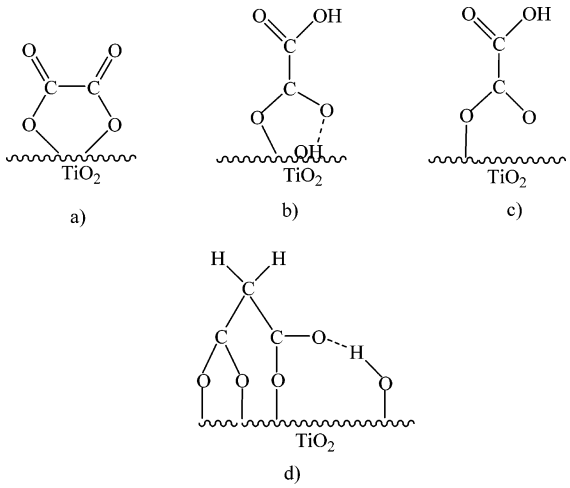

strongly adsorbed species (with a Langmuir adsorption constant $\log(K_L)$ of 6.1−6.6)[11] showed a band at 1690 cm^{-1} and a shoulder slightly above 1700 cm^{-1}. Furthermore, the same species exhibited a band at 1421 cm^{-1} and a weaker one at 1275 cm^{-1}. The reported spectrum[11] matches perfectly the one shown in Figures 3f and 6 (4 → 5), and the species that is formed upon irradiation of malonic acid adsorbed on TiO_2 can be attributed to adsorbed oxalate. The bands at 1421 and 1275 cm^{-1} are therefore assigned to ν(C−O) + ν(C−C) and ν(C−O) + δ(O−C═O) vibrations.[33] The appearance of two bands around 1700 cm^{-1} reveals two groups with C═O character, which suggests an adsorption geometry as shown in Chart 1a. In this form of the oxalate the two C═O groups may be equivalent (depending on the surrounding), and the two distinct vibrational bands in the spectrum correspond to the symmetric and antisymmetric C═O stretching vibration.

Figure 6 shows that more than one species absorbing above 1700 cm^{-1} are present on the TiO_2 surface after illumination (compare 3 → 4 with 4 → 5 in Figure 6). Once formed under band gap illumination of TiO_2 from adsorbed malonic acid these species disappear at different rates from the surface in the dark, which allows distinguishing between them. The faster disappearing species has one absorption band above 1700 cm^{-1} (Figure 6, 3 → 4), whereas the slower disappearing species has two bands (Figure 6, 4 → 5). As discussed above the latter species is assigned to oxalate adsorbed as shown in Chart 1a. The species associated with the band at 1711 cm^{-1} (Figure 6, 3 → 4) is assigned to oxalate in a different adsorption mode. The exact nature of this species is less clear, but likely only one carboxylate group is interacting with the surface in this case (see Chart 1, parts b and c). The band above 1700 cm^{-1} is then ascribed to the ν(C═O) vibration of the protonated acid group. The analysis of ATR-IR spectra of oxalate adsorbed on TiO_2 by singular value decomposition resulted, in addition to the strongly adsorbed oxalate species, in two different species with only one absorption band above 1700 cm^{-1} (with Langmuir constants $\log(K_L)$ of 4.4−5.6 and 3−3.5, respectively).[31,33] The observed band in Figure 6 (3 → 4) is compatible with the reported spectra for the more strongly bound of these two species, which has a band slightly above 1710 cm^{-1}. For this species an adsorption geometry as shown in Chart 1, parts b or c, has been proposed.[31] Note that this assignment implies that the acid group which is not bound to the surface is protonated.

Adsorption Mode of Malonic Acid. Previously the vibrational band at 1430 cm^{-1} of adsorbed malonic acid was ascribed to a $\delta(CH_2)$ mode.[33,34] This mode may indeed bear some $\delta(CH_2)$ character, but the observation of the same band in the spectrum of deuterated malonate (Figure 4) clearly shows that it has to be assigned primarily to a $\nu_s(COO^-)$ mode. The four bands observed at 1625, 1575, 1430, and 1362 cm^{-1} for deuterated malonate on TiO_2 (Figure 4a) are assigned to $\nu_{as}(COO^-)$ (former two bands) and $\nu_s(COO^-)$ (latter two bands) vibrations. This is evidence for quite different carboxylate groups, which may have several origins. First of all P25 is a mixture of anatase (80−90%) and rutile (10−20%), and the two sets of carboxylate bands could originate from adsorption on the two crystal phases. We can exclude this possibility as the spectrum of malonic acid adsorbed on P25 strongly resembles the spectrum of malonic acid on anatase.[35] Another possibility which could lead to two sets of carboxylate bands would be the presence of two distinctly different adsorbed species. From ATR-IR spectra at different pH values and on the basis of a singular value decomposition it was concluded that the adsorption of malonic acid on TiO_2 can very well be described by only one adsorbed species.[35] All the bands observed in Figure 4a therefore belong to the same adsorbed species, which shows that the two carboxylate groups within the adsorbed molecule are largely different.

The wavenumber difference Δ between the $\nu_{as}(COO^-)$ and $\nu_s(COO^-)$ modes is diagnostic for the coordination mode of the carboxylate.[33,36−38] If this difference for the adsorbed carboxylate is larger than for the dissolved carboxylate then the coordination mode is monodentate.[36] If Δ is smaller for the adsorbed species than for the dissolved one then chelating and/or bridging coordination is indicated. Obviously, for the two pairs of carboxylate vibrations in the spectrum of adsorbed malonic acid two different combinations are possible with Δ values of either 263 and 145 cm^{-1} or 213 and 195 cm^{-1}, whereas for dissolved malonic acid Δ = 209 cm^{-1} (Figure 2). We prefer the former of the two possibilities, as the spectrum indicates largely different coordination for the two carboxylate groups, and propose an adsorption mode with one monodentate (large Δ) and one bidentate/chelating carboxylate as shown in Chart 1d.

Qualitative Considerations. From Figure 5 some qualitative considerations on relative reaction rates and coverage can be made. Under our conditions the coverage of malonic acid under irradiation is only about 25% of its value in the dark (Figure 5, regimes 1 and 2). Upon irradiation malonic acid reaches almost steady-state coverage after about 5 min, whereas it takes at least 20 min for oxalic acid to reach steady state. This indicates that the transformation of malonic acid into oxalic acid is not the only surface reaction that is occurring. Oxalic acid is reacting further under illumination, and malonic acid is constantly desorbing from the surface. Furthermore reaction pathways that do not involve oxalic acid may be possible (see later).

Figure 5 shows that the photoassisted degradation of oxalic acid is very fast (regime 5, 50% depletion of adsorbed oxalic acid in about 1 min). The fact that during continuous illumination and flow of malonic acid the intermediate oxalic acid is observed on the TiO_2 surface means that the formation of oxalic acid (and therefore the photoassisted reaction of malonic acid) is also fast. An estimate for the relative rates can be made as follows. Figure 5 shows that readsorption of malonic acid after illumination results in a coverage of only about 85% of its value before illumination (regime 3 in Figure 5). The remaining 15% of surface sites are occupied by oxalic acid at this point (regime

SCHEME 1: Proposed Reaction Mechanism for Photoassisted Mineralization of Malonic Acid over TiO_2

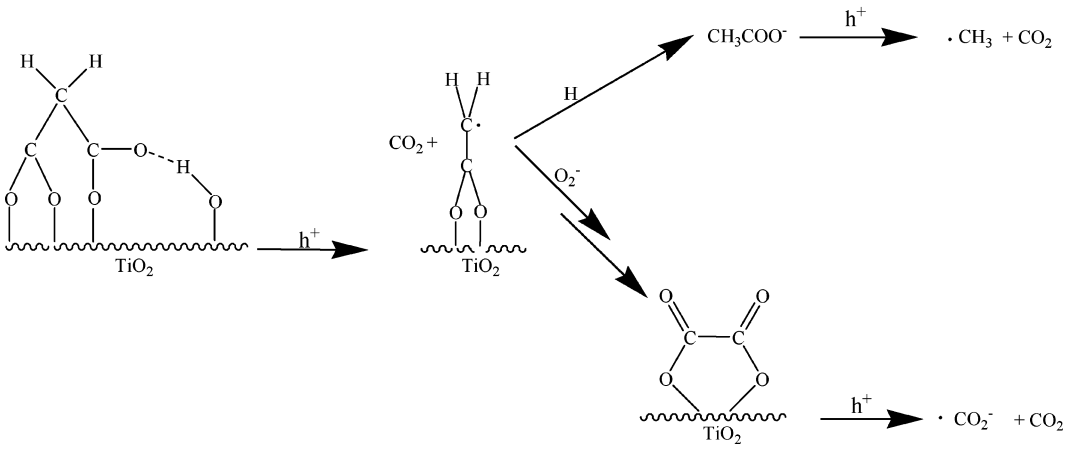

3), which cannot be displaced by malonic acid. As most of the oxalic acid is desorbing very slowly, this coverage corresponds approximately to the steady-state oxalic acid coverage under illumination (regime 2). Under illumination in the steady-state malonic acid reaches only 25% of full coverage (first adsorption in the dark). From the steady-state condition for oxalic acid under illumination one can estimate the relative rate constants for photoassisted reaction of oxalic acid (k_{OA}) and of malonic acid for the pathway leading to oxalic acid (k_{MA}): $k_{OA}/k_{MA} = \theta_{MA}/\theta_{OA} \approx 0.25/0.15 = 1.67$, where θ_{MA} and θ_{OA} are the steady-state coverage of malonic acid and oxalic acid, respectively. The rate constant for oxalic acid is slightly larger than the one for malonic acid. It should be pointed out that the overall reaction rate for malonic acid photoassisted degradation may be larger due to other possible pathways that do not go through oxalic acid.

Another important conclusion emerging from the analysis of Figure 5 is that under illumination the surface is largely depleted from adsorbed acid (malonic and oxalic acid). As no other species are observed in significant amount it is concluded that under illumination a large fraction of the surface (about 60%) is not covered with adsorbate. Difference spectrum 2 → 3 in Figure 6 reveals the spectral changes upon switching off the light in the presence of dissolved malonic acid. Two weak positive features around 1700 cm^{-1} can be observed. The increase of these bands in the dark is somehow surprising because significant bands around 1700 cm^{-1} were never observed to grow in the dark under any other condition. Close inspection reveals that the maxima of the two bands are not identical to the maxima of the bands associated with strongly adsorbed oxalic acid (see difference spectrum 1 → 2 in Figure 6). In fact, at the position of the latter bands, as indicated by the vertical lines in Figure 6, minima are observed in the difference spectrum 2 → 3. The observed features can be explained by a restructuring of the adsorbed oxalic acid, from structure a in Chart 1, responsible for the negative bands at 1708 and 1690 cm^{-1}, into structure b or c in Chart 1, responsible for the broad band at 1711 cm^{-1}. This observation furthermore shows that the steady-state distribution of adsorption modes of oxalic acid under irradiation does not correspond to the equilibrium distribution in the dark.

After illumination and in the presence of dissolved malonic acid the ATR-IR spectrum stabilizes after some time (Figure 5, regime 3). Under these conditions oxalic acid remains on the surface. However, the change from dissolved malonic acid toward water flow leads to a decrease of the signal at 1711 cm^{-1} (see Figure 6, 3 → 4) that we assign to weakly adsorbing oxalic acid (Chart 1, parts b and c). This could be explained either by desorption of this species from the TiO_2 surface or by a deprotonation of the free (not surface bound) acid group. We prefer the latter interpretation. At pH 3.5 the free acid group of adsorbed oxalic acid (Chart 1, parts b and c) is expected to be protonated, whereas at neutral pH in pure water it is expected to be deprotonated. Note that the pK_a values of dissolved oxalic acid are 1.23 and 4.19.[32] This view is corroborated by Figure 7 (corresponding to regime 5 in Figure 5), where a surface that mainly contains adsorbed oxalic acid is illuminated in water. Spectrum (b) in Figure 7, and to a minor extent spectrum (c), reveals a broad band centered at 1580 cm^{-1}, which we assign to the deprotonated form of weakly adsorbed oxalic acid (Chart 1, parts b and c). Dissolved deprotonated oxalic acid in solution is characterized by a broad $\nu_{as}(COO^-)$ band at 1570 cm^{-1}.[33] It has been proposed before that under band gap illumination the weakly adsorbed oxalate species (Chart 1, parts b and c) are transformed to strongly adsorbed oxalate (structure a in Chart 1), which is then undergoing photoassisted degradation.[31] In the latter study, however, the experiments were performed at pH values, at which the weakly bound oxalic acid (Chart 1, parts b and c) was protonated.

Mechanism of Photoassisted Mineralization of Malonic Acid on TiO_2. The primary initial reaction mechanism for strongly adsorbed carboxylic acid is a photo-Kolbe reaction, initiated by a photogenerated hole. This leads to CO_2 and a carbon-centered radical. The fate of this radical may be more complex. The radical can abstract a hydrogen atom from any other suitable molecule, which would lead to acetic acid. Acetic acid only weakly adsorbs on TiO_2 (Langmuir constant of log(K_L) = 2.2[39]) and is therefore expected to desorb readily from the surface. There is no sign in the ATR-IR spectra of adsorbed acetic acid, which is characterized by a strong band slightly above 1500 cm^{-1}.[39] The carbon-centered radical can also react with oxygen to the corresponding peroxyl radical, which may then ultimately be transformed to a carboxylic acid,[40] in our case oxalic acid, which is observed in the ATR-IR spectra. Adsorbed oxalate ($^-OOC-COO^-$) can further react with a photogenerated hole (photo-Kolbe reaction) to form CO_2 and a $CO_2^{\bullet -}$ radical. The latter ultimately also leads to CO_2, possibly via the formation of formic acid.[41] Scheme 1 summarizes the discussed reaction mechanism.

ATR-IR technique as applied here is sensitive to the processes taking place at the solid−liquid interface, and the investigation shows that oxalic acid is an intermediate during the photoassisted mineralization of malonic acid. Oxalic acid is desorbing slowly and mineralized fast, which implies that the concentration of

oxalic acid in solution is small, despite the fact that it is a major intermediate in the mineralization of malonic acid. Indeed, in the photoassisted degradation of fumaric and maleic acid oxalic acid was observed only in very small amount in solution.[41] These considerations indicate that care must be taken when reaction mechanisms are derived from dissolved intermediates, because intermediates on the catalytic surface may not be observed in large quantities in solution but still play a major role.

Conclusions

The photoassisted mineralization of malonic acid on P25 TiO_2 can be followed in situ by ATR-IR spectroscopy. Upon illumination the coverage of adsorbed malonic acid is decreasing and oxalic acid is observed on the TiO_2 surface. Under illumination a large fraction of the surface is free from adsorbed acid. The transient behavior of malonic and oxalic acid observed on the catalyst surface upon illumination indicates other reaction pathways for malonic acid decomposition not involving oxalic acid. Because oxalic acid desorption from the TiO_2 surface is slow, its concentration in solution is low despite the fact that it is a major intermediate in the decomposition of malonic acid. This indicates that care must be taken when deriving reaction mechanisms and pathways based only on stable intermediate species observed in solution.

Acknowledgment. Funding by the Swiss National Science Foundation is kindly acknowledged.

References and Notes

(1) Fujishima, A.; Honda, K. *Nature* **1972**, *238*, 37.
(2) Khan, S. U. M.; Al-Shahry, M.; Ingler, W. B. *Science* **2002**, *297*, 2243.
(3) Wang, R.; Hashimoto, K.; Chikuni, M.; Kojima, E.; Kitamura, A.; Shimohigashi, M.; Watanabe, T. *Nature* **1997**, *388*, 431.
(4) Asahi, R.; Morikawa, T.; Ohwaki, T.; Aoki, K.; Taga, Y. *Science* **2001**, *293*, 269.
(5) Hoffmann, M. R.; Martin, S. T.; Choi, W. Y.; Bahnemann, D. W. *Chem. Rev.* **1995**, *95*, 69.
(6) Linsebigler, A. L.; Lu, G.; Yates, J. T. *Chem. Rev.* **1995**, *95*, 735.
(7) Szczepankiewicz, S. H.; Colussi, A. J.; Hoffmann, M. R. *J. Phys. Chem. B* **2000**, *104*, 9842.
(8) Draper, R. B.; Fox, M. A. *Langmuir* **1990**, *6*, 1396.
(9) Kesselman, J. M.; Weres, O.; Lewis, N. S.; Hoffmann, M. R. *J. Phys. Chem. B* **1997**, *101*, 2637.
(10) Harrick, N. J. *Internal Reflection Spectroscopy*; Interscience Publishers: New York, 1967.
(11) Hug, S. J.; Sulzberger, B. *Langmuir* **1994**, *10*, 3587.
(12) Tejedor-Tejedor, M. I.; Yost, E. C.; Anderson, M. A. *Langmuir* **1990**, *6*, 979.
(13) Connor, P. A.; Dobson, K. D.; McQuillan, A. J. *Langmuir* **1995**, *11*, 4193.
(14) Bürgi, T.; Baiker, A. *J. Phys. Chem. B* **2002**, *106*, 10649.
(15) Ferri, D.; Bürgi, T. *J. Am. Chem. Soc.* **2001**, *123*, 12074.
(16) Bürgi, T. *J. Catal.* **2005**, *229*, 55.
(17) Bürgi, T.; Bieri, M. *J. Phys. Chem. B* **2004**, *108*, 13364.
(18) Bürgi, T.; Wirz, R.; Baiker, A. *J. Phys. Chem. B* **2003**, *107*, 6774.
(19) Keresszegi, C.; Ferri, D.; Mallat, T.; Baiker, A. *J. Catal.* **2005**, *234*, 65.
(20) Ortiz-Hernandez, I.; Williams, C. *Langmuir* **2003**, *19*, 2956.
(21) Ortiz-Hernandez, I.; Owens, D. J.; Strunk, M. R.; Williams, C. T. *Langmuir* **2006**, *22*, 2629.
(22) Hamminga, G. M.; Mul, G.; Moulijn, J. A. *Chem. Eng. Sci.* **2004**, *59*, 5479.
(23) He, R.; Davafa, R. R.; Dumesic, J. A. *J. Phys. Chem. B* **2005**, *109*, 2810.
(24) Ebbesen, S. D.; Mojet, B. L.; Lefferts, L. *Langmuir* **2006**, *22*, 1079.
(25) Nakamura, R.; Imanishi, A.; Murakoshi, K.; Nakato, Y. *J. Am. Chem. Soc.* **2003**, *125*, 7443.
(26) Nakamura, R.; Nakato, Y. *J. Am. Chem. Soc.* **2004**, *126*, 1290.
(27) Warren, D. S.; McQuillan, A. J. *J. Phys. Chem. B* **2004**, *108*, 19373.
(28) Kesselman-Truttmann, J. M.; Hug, S. J. *Environ. Sci. Technol.* **1999**, *33*, 3171.
(29) Ekström, G. N.; McQuillan, A. J. *J. Phys. Chem. B* **1999**, *103*, 10562.
(30) Araujo, P. Z.; Mendive, C. B.; Rodenas, L. A. G.; Morando, P. J.; Regazzoni, A. E.; Blesa, M. A.; Bahnemann, D. *Colloids Surf., A* **2005**, *265*, 73.
(31) Mendive, C. B.; Bahnemann, D. W.; Blesa, M. A. *Catal. Today* **2005**, *101*, 237.
(32) Smith, R. M.; Martell, A. E. *Critical Stability Constants*; Plenum Press: New York, 1979.
(33) Dobson, K. D.; McQuillan, A. J. *Spectrochim. Acta* **1999**, *A55*, 1395.
(34) Schmelz, M. J.; Nakagawa, I.; Mizushima, S.-I.; Quagliano, J. V. *J. Am. Chem. Soc.* **1959**, *81*, 287.
(35) Hug, S.; Bahnemann, D. *J. Electron Spectrosc. Relat. Phenom.* **2006**, *150*, 208.
(36) Deacon, G. B.; Phillips, R. J. *Coord. Chem. Rev.* **1980**, *33*, 227.
(37) Mehrota, R. C.; Bohra, R. Vibrational spectra. In *Metal Carboxylates*; Academic Press: New York, 1983; p 48.
(38) Ferri, D.; Bürgi, T.; Baiker, A. *Helv. Chim. Acta* **2002**, *85*, 3639.
(39) Rotzinger, F. P.; Kesselman-Truttmann, J. M.; Hug, S.; Shklover, V.; Grätzel, M. *J. Phys. Chem. B* **2004**, *108*, 5004.
(40) von Sonntag, C.; Schuchmann, H. P. *Angew. Chem, Int. Ed.* **1991**, *30*, 1229.
(41) Franch, M. I.; Ayllon, J. A.; Domènech, X. *Catal. Today* **2002**, *76*, 221.